Rapid and Green Synthesis of Silver Nanoparticles via Sodium Alginate Media

Sepideh Keshan Balavandy[1], Kamyar Shameli[2,*], Zurina Zainal Abidin[1,3,*]

[1]Advanced Materials and Nanotechnology Laboratory, Institute of Advanced Technology (ITMA), Universiti Putra Malaysia, 43400 UPM Serdang, Selangor, Malaysia
[2] Malaysia-Japan International Institute of Technology (MJIIT), Universiti Teknologi Malaysia, 54100, Malaysia
[3] Department of Chemical and Environmental Engineering, Faculty of Engineering, University Putra Malaysia, 43400 UPM Serdang, Selangor
[*]E-mail: kamyarshameli@gmail.com, zurina@eng.upm.edu.my

This study focuses on influence of accelerator in rapidly and green synthesis of silver nanoparticles (Ag-NPs) with the natural polymeric matrix. Silver nitrate, sodium alginate (Na-Alg) and sodium hydroxide have been used as silver precursor, stabilizer/reducing agent, and accelerator reagent, respectively. The resulting products have been confirmed to be Ag-NPs smaller than 20 nm using powder X-ray diffraction (PXRD), UV-visible spectroscopy (UV-vis), Fourier transform infrared (FT-IR) spectroscopy as well as transmission electron microscopy (TEM) and scanning electron microscopy. The colloidal solutions of Ag-NPs obtained at different volumes of NaOH show strong and different surface plasmon resonance (SPR) peaks, which can be explained from the TEM images of Ag-NPs and their particle size distribution. Compared with other synthetic methods, this work is rapid, green and simple to use. The newly prepared Ag-NPs may have many potential applications in chemical pharmaceutical and food industries.

1. INTRODUCTION

Nanotechnology is a multidisciplinary research field that emerges from physical, chemical, and engineering sciences with novel techniques and produces material at nanoscale level [1]. Nowadays, nanomaterials have been improved as essential building elements of nanotechnology. Since the particle size can be controlled readily from 1 nm to 100 nm in diameter they exhibit larger surface area to volume ratio [2]. This increase in surface area to volume ratio leads to the change of the electrical,

optical, magnetic and chemical properties of nanoparticles better than the bulk materials [3–5]. Noble metals such as Ru, Pd, Au, Pt and especially Ag are exhibiting a particularly wide range of material behavior along the atomic to bulk transition [6].

By applying "green" chemistry rules silver nanoparticles (Ag-NPs) have been widely used during the past few years in various applications, such as biomedicine [7-8], biosensor [9], and catalysis [10] . Ag-NPs synthesized by various methods such as physical, chemical, and biological methods. Physically and chemically mediated synthesis necessitate high pressure and temperature, high cost, and toxicity [11], including, γ-Ray [12, 13], UV-irradiation [14], microwave irradiation [15] and chemical reduction [16, 17]. Polymers [18] have also been used as well as bacteria [19], fungi [20, 21], algae [22] and plants [23, 24] as stabilizers to provide stability for the metal nanoparticles against oxidation, agglomeration, and precipitation additionally have some advantage more than conventional methods.

Preparations of Ag-NPs in various polymers have been studied to give well-dispersed Ag-NPs, such as polyethylene glycol [25, 26], polyvinylpyrrolidine (PVP) [27], polyaniline [28], poly(methyl methacrylate) [29], polyacrylonitrile (PAN) [30] and poly (vinyl alcohol) [31]. Natural polymers have also been published because they are non-toxic and biocompatible. For example, natural rubber [32], polysaccharides [33], tripeptide (glutathione) [34], cellulose [35] and chitosan [36] have been used as matrices or stabilizers for preparation of metallic nanoparticles.

The unique chemical and physical properties of nanoparticles make them extremely suitable for designing new and improved sensing devices, especially electrochemical sensors and biosensors. Many kinds of nanoparticles, such as metal, metal oxide and semiconductor nanoparticles have been used for constructing electrochemical sensors and biosensors, and these nanoparticles play different roles in different sensing systems. The important functions provided by nanoparticles include the immobilization of biomolecules, the catalysis of electrochemical reactions, and the enhancement of electron transfer between electrode surfaces and proteins, labeling of biomolecules and even acting as reactant [37].

We reported here the use of medicinal valuable polymer as the stabilizing agent and use aqueous solution of NaOH as an either reducing agent or accelerator in the rapid synthesis of metallic nanoparticles e.g., Ag [38]. Sodium alginate (Na-Alg) is a natural polymer extracted from the cell walls of brown seaweed and has good biocompatibility and biodegradability. in recent years, it has been widely used in water purification [39], catalysis [40], wound dressings [41, 42], drug carriers and tissue scaffolds [43, 44]. This work is on the synthesis of Ag-NPs by a simple and rapid chemical process for preparing well-dispersed Ag-NPs in natural polymeric media. The using Na-Alg as a capping agent and NaOH as a reducing agent and accelerator simultaneously. The morphologies of Ag-NPs and the mechanism of their formation by oxidation of Na-Alg using an accelerator reagent are discussed.

2. MATERIALS AND METHOD

All chemicals and reagents in this effort were of analytical grade and used as received without any further purification. Materials used for the synthesis of Ag-NPs included silver nitrate 99.98%

from Acros (New Jersey, USA) as a silver precursor, sodium alginate Acros (New Jersey, USA) for analysis was used as a green substrate to Ag atoms, and sodium hydroxide powder 98.5% Sigma-Aldrich (USA) as an accelerator. All solution was freshly prepared using Double distilled water.

2.1 Synthesis of Silver Nanoparticles

In the present study, the preparation of Ag-NPs in the Na-Alg matrix is quite directly forward. In a typical synthesis 125 mL of Na-Alg (1.5 wt %) was added to a 125 mL aqueous solution of $AgNO_3$ (0.05 M) in a flask to obtain the complex of silver ion with substrate $[Ag(Na-Alg)]^+$. The obtain solutions were distributed into five cuvettes under stirring, and heated up to 60 °C, then different volumes of aqueous solution of NaOH (1 M) were added to each prepared 50 mL cuvettes solution [0.5, 1.0, 1.5, 5 and 10 mL (S1–S5)]. The colour of reactions immediately turned from colourless to dark brown in all samples that indicate the formation of [Ag(Alg)] nanoparticles. The reaction was continued for 15 minutes. The obtained colloidal suspensions were then centrifuged at 20,000 rpm for 15 min, these precipitate were washed three times using double distilled water in order to remove the silver ion residue and dried overnight at 40 °C under a vacuum.

2.2 Characterization Methods and Instruments

The prepared Ag-NPs were characterized using ultraviolet-visible (UV-vis) spectroscopy, transmission electron microscopy (TEM), scanning electron microscopy (SEM), Fourier transform infrared (FT-IR) spectroscopy and powder X-ray diffraction (PXRD). The UV-vis spectra were recorded over the range of 300-700 nm with a Lambda 35-Perkin Elmer UV-vis spectrophotometer. TEM observations were conducted using a Hitachi H-7100 electron microscope while the particle size distribution was determined using the UTHSCSA Image Tool version 3.00 program. The SEM was performed using the Philips XL-30 instrument to study the morphology of Na-Alg and Ag(Alg)-NPs. The FT-IR spectra were recorded over the range of 400–4000 cm^{-1} utilizing the Series 100 Thermo Nicolet spectrophotometer. The structure of produced Ag-NPs has been studied using powder X-ray diffraction (PXRD, Philips, X'pert, Cu Kα). PXRD patterns were recorded at a scan speed of 2°/min. After reactions, the samples were centrifuged using a high-speed centrifuge machine (Avanti J25, Beckman).
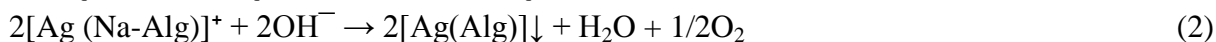
3. RESULT AND DISSCUTION

In this research, a convenient and "green" chemical reduction procedure was put forward for the reduction of Ag (I) onto Na-Alg colloidal solution. Sodium alginate has a large abundance of carboxylate(−COO) and hydroxyl (−OH) functionalities, which helps them to act as both a reduction and a stabilizer [45]. As shown hydroxyl (−OH) and carboxylate (−COO) groups of Na-Alg as a capping agent can form bonding with the surface of Ag-NPs. This is due to the surface of Ag-NPs which is positively charge. Extensively, we suppose that colloidal stabilization for [Ag(Alg)] occur due

to the presence of van der waals forces between the negatively partial charges of hydroxyl and acetyl groups that present in the molecular structure of the Alg, with positive charge of Ag-NPs that surround on the surface of NPs. Figure 1 illustrates the interaction between the charged Ag-NPs and Na-Alg structures with surface positive charges of Ag-NPs [46].
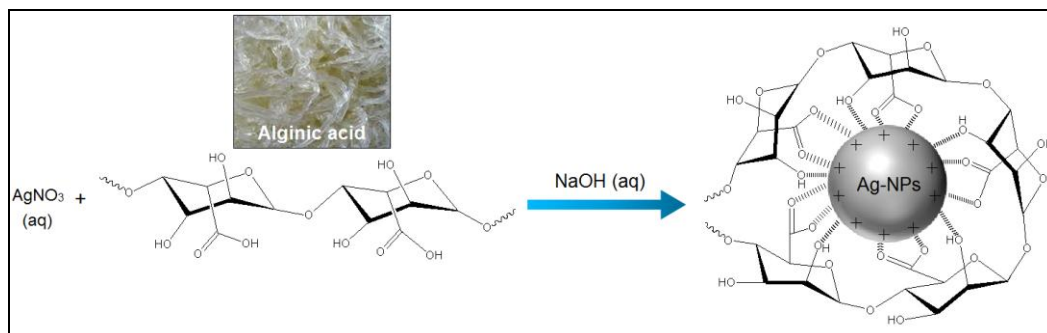
Figure 1. Schematic illustration show the interactions between negative charges of carboxyl and hydroxyl groups of alginate ions with positive charges of Ag-NPs surface.

Earlier literature documents that Ag (I) and Au (III) ions can lead to aggregated Ag and Au-NPs if kept in contact with alginate for long periods of time [47]. In the current approach, pH control agglomeration technique helps such a reduction to occur within a short time period (30 min) to lead to Ag embedded in Na-Alg substrate. The chemical reaction for the formation of Ag-NPs is:

$$Ag^+_{(aq)} + Na\text{-}Alg_{(aq)} \rightarrow [Ag\,(Na\text{-}Alg)]^+_{(aq)} \qquad (1)$$
$$2[Ag\,(Na\text{-}Alg)]^+ + 2OH^- \rightarrow 2[Ag(Alg)]\downarrow + H_2O + 1/2O_2 \qquad (2)$$

After dispersion of silver ions in the aqueous solution of Na-Alg matrix (Equation 1), Na-Alg reacted with the Ag^+ to form a Na-Alg complex $[Ag(Na\text{-}Alg)]^+$, which further reacts with OH^- ions to form Ag-NPs by the reduction of silver ions through the regeneration of alginic acid (Alg) from sodium alginate (Na-Alg) (Equation 2) [48]. The absorbance of Ag (I) by Na-Alg will depend on the solution pH. Also, during the incorporation, the solution pH may change due to proton exchange. Here in, during the mix of $AgNO_3$ onto the Na-Alg, the pH was ~6 and no pH change was noticed before NaOH adding process. On the other hand, the solution pH increased during the increasing of NaOH, the pH was ~ 6.8, 7.6, 7.7, 11.7 and 12.3 for adding the amount of 0.5, 1, 1.5, 5 and 10 mL of NaOH, respectively.

Figure 2. Photograph of $[Ag(Na\text{-}Alg)]^+$ (S0) and $[Ag(Alg)]$ solution prepare after added of different volume of NaOH (1 M), respectively [0.5 (S1), 1 (S2), 1.5 (S3), 5 (S4) and 10 mL (S5)].

The obtained colloidal Ag-NPs were characterized by spectroscopic results. The formation of Ag-NPs was studied using UV-vis spectroscopy, which has proven to be a very useful technique for the analysis of nanoparticle formation over time. The colour of the obtained samples at different volumes of NaOH rapidly changed from colourless to dark brown, indicating the formation of Ag-NPs (Figure 2). brown colour of the aqueous solution was due to the excitation of the surface plasmon resonance and SPR band which both play an important role in the confirmation of Ag-NPs formation [49].

Nanoparticles formation was dependent on the different physical and chemical factors such as metal ion concentration, incubation time, pH, and temperature. Shape and size of nanoparticles formation are further depending on the pH of solution.

UV-vis absorption spectra of prepared samples are shown in Figure 2. The obtained Ag-NPs displayed absorption peaks and the characteristic surface plasmon resonance (SPR) band of silver, centered from 390 to 410 nm. The location (λ_{max}) of the SPR peaks and volumes of NaOH with corresponding pH are also summarized in Table 1.

Table 1. The characteristics of Ag-NPs prepared at different volumes of NaOH.

Sample	Volume of NaOH	pH	λ_{max}	Mean diameter (nm)
0	-	6.5	-	-
1	0.5	6.8	410	25.85
2	1.0	7.6	404	16.54
3	1.5	7.7	403	12.19
4	5.0	11.7	390	10.96
5	10.0	12.3	387	17.50

3.1 UV-visible Spectroscopy

The formation of Ag-NPs in the Na-Alg media was further determined by using UV-visible spectroscopy, which was shown on the surface plasmon resonance (SPR) bands. The [Ag(Na-Alg)]⁺ peak was not observed before adding NaOH. As indicated, the first addition of NaOH (0.5 mL) led to the broadening of the SPR peak relative to the sample S1. Greater volumes of NaOH (1 and 1.5 mL) increased the absorbance due to increases in silver concentration (S2, S3). Moreover, in sample S4, 5 mL amount of NaOH resulted in a stronger blue-shift in λ_{max} to 390 nm. Previous studies have shown that the spherical Ag-NPs contribute to the absorption bands at around 350 nm in the UV–visible spectra [50]. Generally, the SPR bands are influenced by the size, shape, morphology, composition and dielectric environment of the prepared nanoparticles. The increased volume of accelerator led to the SPR peak being considerably blue-shifted to a lower wavelength. This blue-shift is related to a decrease in the particle size of Ag-NPs [51] because the SPR band in metal nanoparticles displays the blue-shift based on the decreased size of particles. For S5, the λ_{max} was slightly blue-shifted to 387 nm however decrease the absorbance due to the closeness of small size nanoparticles [48-50]. These

results demonstrated good agreement with the results obtained in the TEM images of Ag-NPs and their particle size distribution.
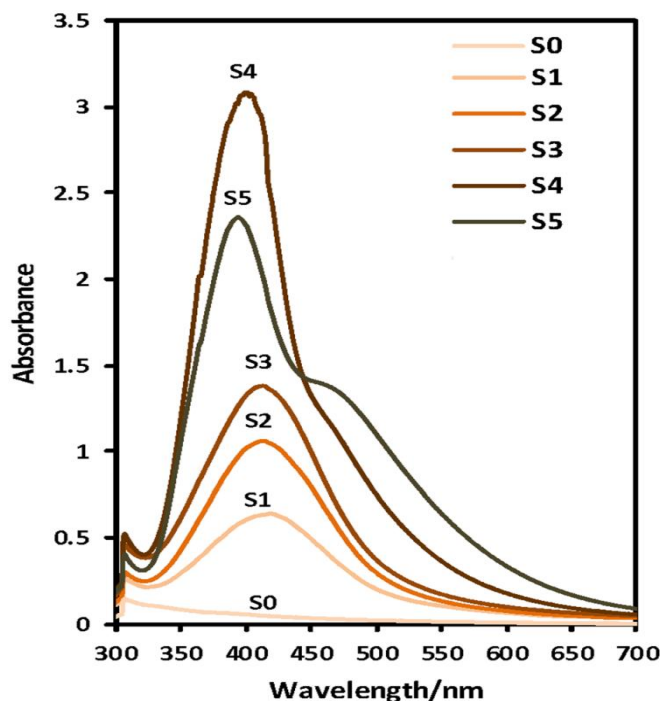

Figure 3. The UV-visible spectra of Ag-NPs prepared in different volumes of NaOH (1M) in Na-Alg mediate.

3.2 Power X-Ray Diffraction Analysis

Figure 4 shows the XRD patterns of Ag-NPs formed at different volumes of NaOH, which indicates the formation of the silver crystalline structure face centered cubic. Moreover, all the Ag-NPs had a similar diffraction profile, and XRD peaks in the wide angler ange of 2θ ($30° < 2\theta < 80°$) point out that the peaks in $38.17°$, $44.28°$, $64.5°$, $77.52°$ and $81.62°$ could be attributed to the 111, 200, 220, and 311 crystallographic planes of the face-centered cubic silver crystals, respectively [52]. For the all samples, the main crystalline phase was silver; no obvious impurities (e.g., Ag_2O) were evident in the PXRD patterns [53]. The average particle sizes of Ag-NPs can be calculated using Debye–Scherrer Equation (3):

$$n = \frac{K\lambda}{\beta \cos\theta} \tag{3}$$

Where K is the Scherrer constant with value from 0.9 to 1 (shape factor), where λ is the X-ray wavelength (1.5418 Å), $\beta 1/2$ is the width of the XRD peak at half height and θ is the Bragg angle. From the *Scherre* equation the average crystallite size of Ag-NPs for 1.0, 1.5, 5.0 and 10.0 mL of NaOH are found to be around 12-18 nm, which are also in line with the observation of the TEM results discussed later.
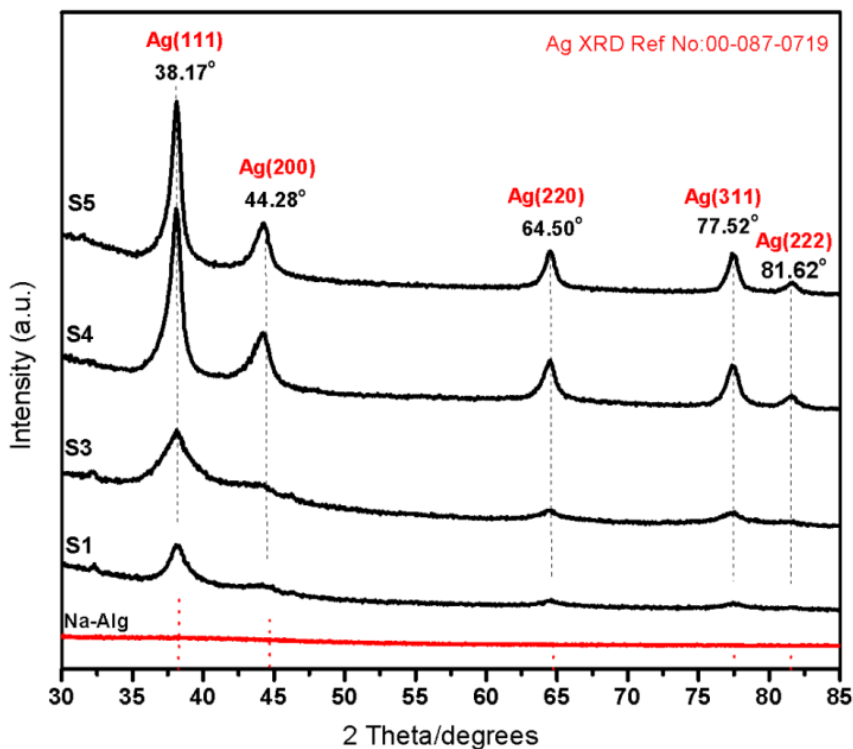
Figure 4. The PXRD patterns of Na-Alg and [Ag(Alg)] prepared at different volumes of NaOH [0.5, 1.5, 5.0 and 10.0 mL (S1, S3, S4, and S5)] respectively.

3.3 Transmission Electron Microscopy

After dispersion of silver ions in the sodium alginate matrix (Equation 1), sodium alginate reacted with the Ag to form stable colloidal suspension complex, and the binding of Ag-NPs by alginate is likely achieved through Ag–O bonding [54].

TEM images and the corresponding particle size distribution of the prepared Ag-NPs in Figure 5 demonstrate the formation of Ag-NPs at different volumes of NaOH. The TEM images and their size distributions revealed that, the mean diameters of Ag-NPs were about 12.19, 10.96 and 17.50 nm for 1.5, 5.0 and 10.0 mL (a–c), respectively. The total numbers of Ag-NPs counted for each TEM images were about 200, 980 and 400 for 1.5, 5.0 and 10.0 mL, respectively. These results approved that addition of NaOH accelerate the reaction, this is due to the proton exchange caused by OH^-, and reducing of $AgNO_3$ solution is favored at higher pH.

However, too much addition of NaOH agglomerated the Ag-NPs in S5. This phenomenon could be due to the fact that, after reaching a certain volume of NaOH particle size growing and the stabilizer was not able to prevent NPs from agglomeration. Furthermore results indicated that the obtained samples retained a narrow particle size distribution that is in accordance with the UV-visible spectra study.
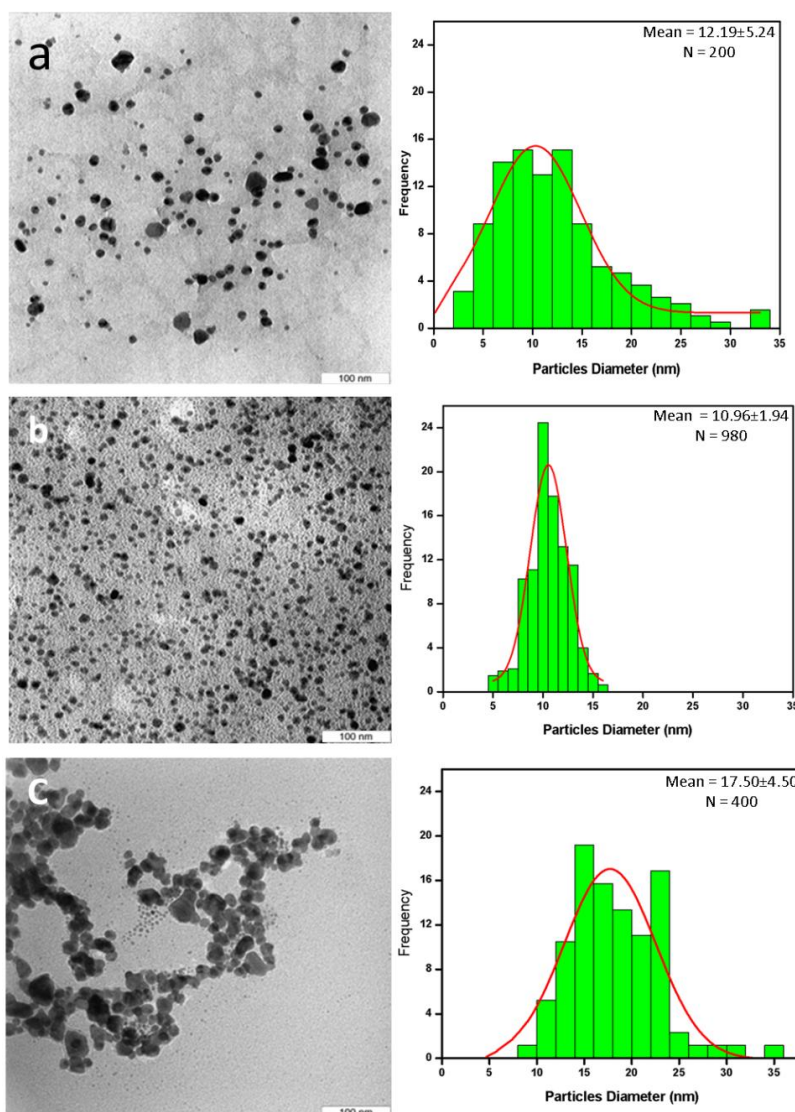
Figure 5. TEM images of Ag-NPs and their particle size distribution at different volumes of NaOH, respectively [1.5, 5.0, and 10.0 mL (a–c)].
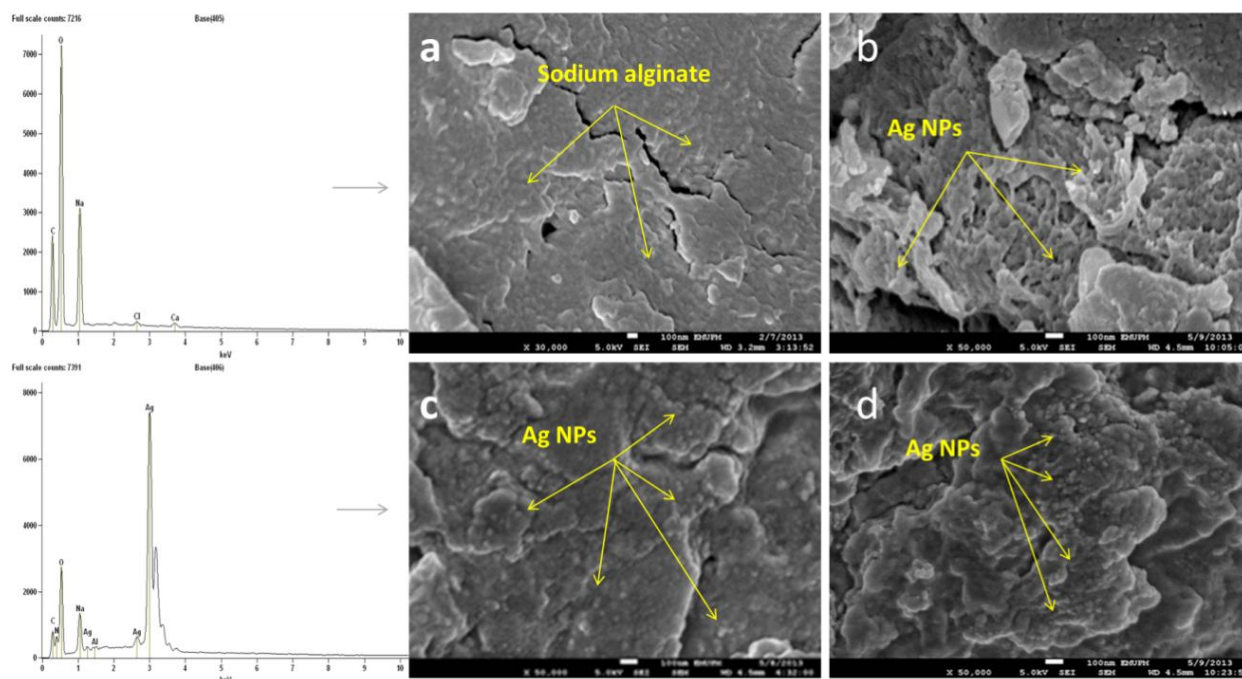
3.2 Scanning Electron Microscopy

The image and EDX spectra of green synthesized Ag-NPs were shown in Figure 6. The FESEM imaging demonstrates the formation of Ag-NPs at the different volume of NaOH, it shows that Ag are nano-spherical with size smaller than 18 and 12 nm for S1 and S4 [Figure 6 (b-c)]. By increase the volume of accelerator to S5, the individual Ag-NPs were agglomerated to form either clusters or large nanoparticles (Figure 6d). This agglomeration took place due to narrow distance between surface of nanoparticles caused by the attractive van der waals force and/or the driving force that tends to minimize the total surface energy of the system [55]. Same result was obtained by TEM images of Ag-NPs.

The exterior surfaces of [Ag(Alg)] due to the presence of small size Ag-NPs become shiny in the spots spherical shapes. Figure 6 also shows the EDX spectra for the Na-Alg and S5. The peaks

around 0.25, 0.5 and 1.1 keV are attributed to elements (C, O and Na) of Na-Alg [56]. The peaks around 2.7, 3.00 and 3.20 keV are related to the silver elements in the [Ag(Alg)].

Figure 6. Scanning electron microscopy of sodium alginate (a), S1 (b), S4 (c) and S5 (d) with respective EDX result.

3.3 FT-IR Chemical Analysis

As shown in Figure 7, FT-IR analysis reveals the functional groups of the Ag-NPs synthesized using sodium alginate and different volume of NaOH. Figure 7 show the peaks of sodium alginate at 3442, 1616, 1303, 1126, 1097 and 950 cm^{-1} are attributed to hydroxyl, C–O–O−,C–O–, C–C, and C–O–C and C–O groups, respectively. They are related to its saccharide structure [57]. The OH stretching vibration bands at 3440 cm^{-1} has shifted to lower frequencies frequently with the increase in NaOH content compared to pure sodium alginate [58]. The reduction of certain peaks is the clear indication of the loss of certain groups. A new band at 1631 cm^{-1} was observed due to the asymmetric stretching of −COO− metal groups, in addition the shift of the band from 1417 to 1384.62 also indicatesthat Na-Alg was doped by NO_3^-. It is due to the stabilization of Ag-NPs by the −COO− group of Na-Alg [40]. Interaction of Ag-NPs with Alg was shown fewer than 850 cm^{-1} spectra; the shifting and disappearing of peaks in the FT-IR spectra of Ag(Alg) clearly indicate the complex between the alginate and Ag-NPs (S3-S5).
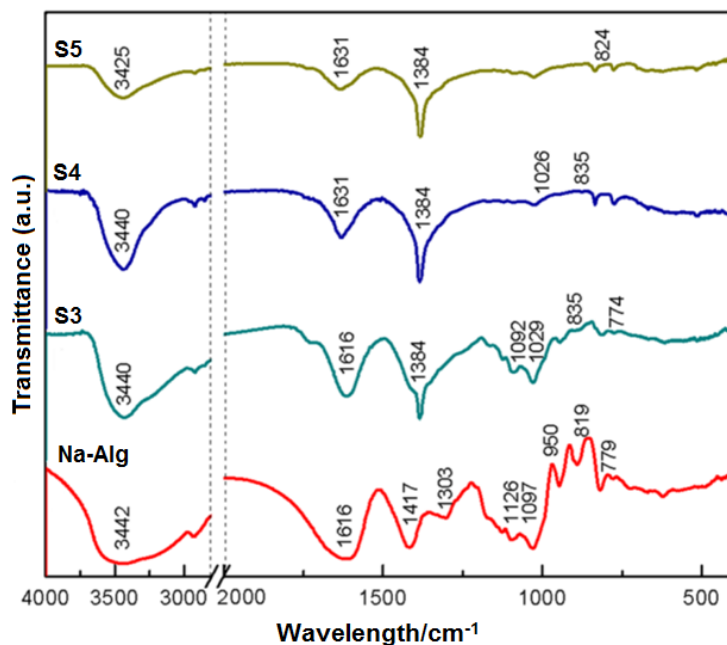
Figure 7. Fourier transforms infrared spectra for Na-Alg and [Ag(Alg)] (S3, S4 and S5), respectively.

4. CONCLUSIONS

We have demonstrated a green and rapid synthesis of high purity Ag-NPs with sodium alginate at different volumes of NaOH as an accelerator for reaction. Smaller volume of NaOH would lead to the formation of nameplates and increasing of NaOH volume was favourable for forming nano-spheres. Nanoparticle agglomeration was controlled with the abundance of functionalities group of sodium alginate as a stabilizing and reducing agent. PXRD and TEM measurements displayed that the resultant nanoparticles were faced centered cubic (fcc) structures and smaller than 20 nm in Diameter. The SEM images demonstrated surface of product without noticeable morphological differences from the initial morphology of them except for appearsspherical shining point due to Ag NPs formation. Moreover, FT-IR suggested that the interactions between Ag-NPs with Na-Alg were strong due to the presence of Ag-O bonding. Thus, this work provides important advantages, namely, simplicity, speed, and eco-friendliness.

References

1. M. Vanaja, G. Gnanajobitha, K. Paulkumar, S. Rajeshkumar, C. Malarkodi, G. Annadurai. *J. Nanostructure Chem*. 3(1) (2013) 1–8.
2. M. Rai, A. Yadav, A. Gade. *Biotechnol. Adv*. 27(1) (2009) 76–83.
3. K.L. Kelly, E. Coronado, L.L. Zhao, G.C. Schatz. *J. Phys. Chem B*. 107 (2003) 668–677.
4. K. Ueda, H. Tabata, T. Kawai. *Appl. Phys. Lett*. 79(7) (2001) 988–990.

5. M.C. Daniel, D. Astruc. *Chem. Rev*. 104(1) (2004) 293–346.
6. T.K. Sau, A.L. Rogach, F. Jäckel, T. Klar, J. Feldmann. *Adv. Mater*. 22(16) (2010)1805–1825.
7. S. Penn. *Curr. Opin. Chem. Biol*. 7(5) (2003) 609–615.
8. D. Schultz. *Curr. Opin. Biotechnol*. 14(1) (2003) 13–22.
9. A.J. Haes, R.P. Van Duyne. *J. Am. Chem. Soc*. 124(35) (2002) 10596–10604.
10. J. Tashkhourian, M.R. Hormozi-Nezhad, J. Khodaveisi, R. Dashti. *Sensors Actuators B Chem*. 158(1) (2011) 185–189.
11. K.S. Kavitha, S. Baker, D. Rakshith, H.U. Kavitha, H.C. Yashwantha Rao, B.P. Harini, S. Satish. *Int. Res. J. Biol. Sci*. 2(4) (2013) 66–76.
12. K. Shameli, M.B. Ahmad,W.M.Z. Wan Yunus, N.A. Ibrahim, Y. Abdollahi. *Int. J. Nanomed.* 5 (2010) 1067–1077.
13. N.M. Huang, S. Radiman, H.N. Lim. *Chem. Eng. J*. 155(1-2) (2009) 499–507.
14. K. Shameli, M.B. Ahmad,W.M.Z. Wan Yunus, A. Rustaiyan, N.A. Ibrahim, M. Zargar, Y. Abdollahi. *Int. J. Nanomed.* 5 (2010) 875–887.
15. S. Kundu, K. Wang, H. Liang. *J. Phys. Chem. C*. 113(1) (2009) 134–141.
16. K. Chou, C. Ren. *Mater. Chem. Phys*. 64 (2000) 241–246.
17. P.K. Khanna, N. Singh, S. Charan, V.V.V.S. Subbarao, R. Gokhale, U.P. Mulik. *Mater. Chem. Phys*. 93(1) (2005)117–121.
18. V.K. Sharma, R. Yngard, Y. Lin. *Adv. Colloid Interface. Sci*. 145(1-2) (2009) 83–96.
19. Mandal D, Bolander ME, Mukhopadhyay D, Sarkar G, Mukherjee P. *Appl Microbiol Biotechnol*. 2006;69(5):485–92.
20. Mohammed Fayaz a, Balaji K, Kalaichelvan PT, Venkatesan R. *Colloids Surf. B. Biointerfaces*. 2009;74(1):123–6.
21. K. Kathiresan, S. Manivannan, M. Nabeel, B. Dhivya. *Colloids Surf. B. Biointerfaces*. 71(1) (2009)133–137.
22. S. Rajeshkumar, C. Kannan, G. Annadurai. *Drag. Invent. Today*. 4(10) (2012) 511–513.
23. M. Zargar, K. Shameli, G.R. Najafi, F. Farahani. *J. Ind. Eng. Chem*. (2014) 1–7.
24. J.Y. Song, B.S. Kim. *Bioprocess. Biosyst. Eng*. 32(1) (2009) 79–84.
25. K. Shameli, M.B. Ahmad, S.D. Jazayeri, P. Shabanzadeh, H. Jahangirian, M, Mahdavi, Y. Abdollahi. *Int. J. Mol. Sci*. 13 (2012) 6639–6650.
26. C. Luo, Y. Zhang, X. Zeng, Y. Zeng, Y. Wang. *J. Colloid Interface Sci*. 288(2) (2005) 444–448.
27. H. Wang, X. Qiao, J. Chen, X. Wang, S .Ding. *Mater. Chem. Phys*. 94(2-3) (2005) 449–453.
28. S. Jing, S. Xing, L. Yu, Y. Wu, C. Zhao. *Mater. Lett*. 61(13) (2007) 2794–2797.
29. H. Kong, J. Jang. *Langmuir*. 24(5) (2008) 2051–2056.
30. Z. Li, H. Huang, T. Shang. *Nanotechnology*. 17(3) (2006) 917–920.
31. Z.H. Mbhele, M.G. Salemane, C.G.C.E. Van Sittert, J.M. Nedeljkovic, V. Djokovic, A.S. Luyt. *Chem. Mater*. 15(25) (2003) 5019–5024.
32. N.H.H. Abu Bakar, J. Ismail, M. Abu Bakar. *Mater. Chem. Phys*. 104(2-3) (2007) 276–283.
33. N.M. Huang, H.N. Lim, S. Radiman. *Colloids Surfaces A Physicochem. Eng. Asp*. 353(1) (2010) 69–76.
34. S.K. Balavandy, K. Shameli, D.R.B.A. Biak, Z.Z. Abidin. *Chem. Cent. J*. 8(1) (2014) 1–11.
35. S. Padalkar, J.R. Capadona, S.J. Rowan. *Langmuir*. 26(11) (2010) 8497–502.
36. M.B. Ahmad, M.Y. Tay, K. Shameli, M.Z. Hussein, J.J. Lim. *Int. J. Mol. Sci*. 12(8) (2011) 4872–4884.
37. C. Batchelor-McAuley, K. Tschulik, C.C.M. Neumann, E. Laborda, R.G. Compton. *Int. J. Electrochem. Sci*. 9 (2014) 1132–1138.
38. M. Singh, I. Sinha, R.K. Mandal. *Mater. Lett*. 63(3-4) (2009) 425–427.
39. S. Lin, R. Huang, Y. Cheng, J. Liu, B.L.T. Lau, M.R. Wiesner. *Water Res*. 47(12) (2013) 3959–3965.
40. J. Yang, J. Pan. *Acta Mater*. 60(12) (2012) 4753–4758.

41. I. Yuvarani, S.S. Kumar, J. Venkatesan, S.K. Kim, P.N. Sudha. *J. Biomater. Tissue Eng*. 2(1) (2012) 54–60.
42. P. Marie Arockianathan, S. Sekar, S. Sankar, B. Kumaran, T.P. Sastry. *Carbohydr Polym*. 90(1) (2012) 717–724.
43. C.H. Goh, P.W.S. Heng, L.W. Chan. *Carbohydr Polym*. 88(1) (2012) 1–12.
44. M. George, T.E. Abraham. *J. Control. Release*. 114(1) (2006) 1–14.
45. A. Pal, K. Esumi, T. Pal. *J. Colloid Interface Sci*. 288(2) (2005) 396–401.
46. B. Baruwati, V. Polshettiwar, R.S. Varma. *Green Chem*. 11(7) (2009) 926.
47. E. Torres, Y.N. Mata, M.L. Blázquez, J. Muñoz, F. González, A. Ballester. *Langmuir*. 21(17) (2005) 7951–7958.
48. R. Paper, R. Vasireddy, R. Paul, A.K. Mitra. *Nanomater. Nanotechnol*. 2 (2012) 1–6.
49. C. Krishnaraj, E.G. Jagan, S. Rajasekar, P. Selvakumar, P.T. Kalaichelvan, N. Mohan. *Colloids Surf. B. Biointerfaces*. 76(1) (2010) 50–56.
50. K. Shameli, M.B. Ahmad, E.A.J. Al-Mulla, P. Shabanzadeh, S. Bagheri. *Res. Chem. Intermed*. (2013) 1–13.
51. J.R. Heath. *Phys. Rev. B*. 40(14) (1989) 9982–9985.
52. S.R. Aragon, M. Elwenspoek. *J. Chem. Phys*. 77 (1982) 3406–3413.
53. P. Raveendran, J. Fu, S.L. Wallen. *J. Am. Chem. Soc*. 125(46) (2003) 13940–13941.
54. Y. Liu, S. Chen, L. Zhong, G. Wu. *Radiat. Phys. Chem*. 78(4) (2009) 251–255.
55. K. Shameli, M.B. Ahmad, P. Shabanzadeh, E.A.J. Al-Mulla, A. Zamanian, Y. Abdollahi, S.D. Jazayeri, M. Eili, F. Aziz Jalilian. *Res. Chem. Intermed*. 40(3) (2014) 1313–1325.
56. H. Bar, D.K. Bhui, G.P. Sahoo, P. Sarkar, S.P. De, A. Misra. *Colloids Surfaces A Physicochem Eng. Asp*. 339(1-3) (2009) 134–139.
57. C. Sartori, D.S. Finch, B. Ralph. *Polymer*. 38(1) (1997) 43–51.
58. K. Tarun, N. Gobi. *indian J. fiber Text Res*. 37 (2012) 127–132.